FULL PAPER

Dalton
www.rsc.org/dalton

In-situ X-ray powder diffraction studies of hydrothermal and thermal decomposition reactions of basic bismuth(III) nitrates in the temperature range 20–650 °C †

Axel Nørlund Christensen,[a] Torben René Jensen,[b] Nicola V. Y. Scarlett,[c] Ian C. Madsen,[c] Jonathan C. Hanson[d] and Angela Altomare[e]

[a] *Højkolvej 7, DK-8210 Aarhus V, Denmark*
[b] *Department of Inorganic Chemistry, University of Aarhus, DK-8000 Aarhus C, Denmark*
[c] *CSIRO Minerals, Clayton South, Victoria 3169, Australia*
[d] *Chemistry Department, Brookhaven National Laboratory, Upton, NY 11973, USA*
[e] *CNR ISMEC c/o Dipartimento Geomineralogico, Via Orabona 4, I-70125 Bari, Italy*

Received 8th April 2003, Accepted 18th June 2003
First published as an Advance Article on the web 7th July 2003

The syntheses of basic bismuth(III) nitrates under hydrothermal conditions and their dry decomposition to α-Bi_2O_3 in solid-state reactions was investigated by *in-situ* synchrotron X-ray radiation powder diffraction. Three basic bismuth(III) nitrates with known structures are: $[Bi_6O_4(OH)_4](NO_3)_6{\cdot}4H_2O$, **C**, $[Bi_6O_4(OH)_4](NO_3)_6{\cdot}H_2O$, **D**, and $[Bi_6O_5(OH)_3](NO_3)_5{\cdot}3H_2O$, **A**. They contain the complex ions $[Bi_6O_4(OH)_4]^{6+}$ and $\{[Bi_6O_5(OH)_3]^{5+}\}_2$, respectively. A fourth basic bismuth(III) nitrate, **X**, apparently has the composition $[Bi_6O_{4.5}(OH)_{3.5}](NO_3)_{5.5}{\cdot}H_2O$ according to chemical analysis. The transformation of **C** via **D** to **X**, or of **C** directly to **X** was established in the *in-situ* hydrothermal synthesis. Similarities in the decomposition paths of **C**, **D** and **X** in the solid-state *in-situ* investigations support the above composition indicated for **X**. The compound **A** has a decomposition path different from those of **C**, **D** and **X**. This is consistent with the complex ion $\{[Bi_6O_5(OH)_3]^{5+}\}_2$ in **A**, being different from the complex ion $[Bi_6O_4(OH)_4]^{6+}$ in the other two basic bismuth(III) nitrates. All four compounds have α-Bi_2O_3 as the final decomposition product.

Introduction

A number of basic bismuth(III) nitrates can be obtained via hydrolysis of bismuth(III) nitrate pentahydrate. The compositions of the products obtained in the hydrolysis reactions depend upon the experimental conditions used.[1] The basic bismuth(III) nitrates characterized in single crystal structure analysis contain the complex ion $[Bi_6O_{4+x}(OH)_{4-x}]^{(6-x)+}$ with $x = 0$ or 1, and their composition is well established. Table 1 lists the composition of these basic bismuth(III) nitrates and of other compounds reported in the literature.

The structure of bismuth(III) nitrate pentahydrate contains two $Bi(H_2O)_4(NO_3)_3$ coordination polyhedra, where Bi is coordinated to ten oxygen atoms from three bidentate nitrate ions and four water molecules. There are two additional water molecules in the unit cell. In the hydrolysis of this compound to $[Bi_6O_4(OH)_4](NO_3)_6{\cdot}4H_2O$, **C**, the complex ion $Bi_6O_4(OH)_4^{6+}$ is formed. The compound **C** is converted to $[Bi_6O_4(OH)_4](NO_3)_6{\cdot}H_2O$, **D**, in a solid-state reaction when it is dried at 80 °C for a few hours. The complex ion $[Bi_6O_4(OH)_4]^{6+}$ in these two structures has six bismuth atoms located at the corners of an octahedron, eight oxygen atoms placed perpendicular to the eight triangular surfaces of the octahedron, and the four OH^- groups form the corners of a tetrahedron. The bismuth–bismuth distances are in the range from 3.616(3) to 3.752(3) Å.[4] The structure of **C** contains four of these complex ions in the unit cell, and that of **D** also has four of the complex ions in the unit cell. Figure 1 is a sketch of the structure of **C**.

The compound $[Bi_6O_5(OH)_3](NO_3)_5{\cdot}3H_2O$, **A**, is converted to the compound $[Bi_6O_6(OH)_3](NO_3)_3{\cdot}1.5H_2O$, **B**, in a hydrothermal synthesis at 190 °C.[1] The complex ion $[Bi_6O_5(OH)_3]^{5+}$ in **A** is a distorted version of the equivalent ions in **C** and **D**. In the structure of **A** the complex $[Bi_6O_5(OH)_3]^{5+}$ is seen as an ion with the composition $\{[Bi_6O_5(OH)_3]^{5+}\}_2$ and the unit cell contains two of these complex ions. The reported composition of **B** is questionable. Thermogravimetric analysis of **B** shows loss in weight to α-Bi_2O_3 of 11.5% compared to a calculated value of 13.4% for the suggested formula.

The compound $[Bi_6O_5(OH)_3](NO_3)_5{\cdot}2H_2O$, **X**, was obtained in a previous investigation, where homogeneous hydrolysis of urea was assumed to play an important role in the hydrolysis reactions. The composition of **X** was derived from thermogravimetric analysis. Several attempts have been made to solve the crystal structure of **X**, but single crystal analysis results in models with unrealistically short Bi–Bi distances. The data

† Electronic supplementary information (ESI) available: Figs S1–S8: TGA–TDA and PXRD patterns. See http://www.rsc.org/suppdata/dt/b3/b303926a/

Table 1 Basic bismuth(III) nitrates

Compound	Notation this work	Ref.	ICDD card or ref. to powder pattern
$[Bi_6O_5(OH)_3](NO_3)_5{\cdot}3H_2O$	**A**	2	70–1226
$[Bi_6O_4(OH)_4](NO_3)_6{\cdot}4H_2O$	**C**	3	84–2189
$[Bi_6O_4(OH)_4](NO_3)_6{\cdot}H_2O$	**D**	4,5	71–1360, 70–2235
$[Bi_6O_5(OH)_3](NO_3)_5{\cdot}2H_2O$[a]	**X**	1	Table 3 in ref. 1
$[Bi_6O_4(OH)_4](OH)(NO_3)_5{\cdot}0.5H_2O$[a]	**E**	6	16–504
$[Bi_6O_6(OH)_2](NO_3)_4{\cdot}2H_2O$[a]	**F**	7	28–654
$[Bi_6O_6(OH)_3](NO_3)_3{\cdot}1.5H_2O$[a]	**B**	7	Table 5 in ref. 1

[a] Compositions not confirmed in single crystal structure analysis.

DOI: 10.1039/b303926a

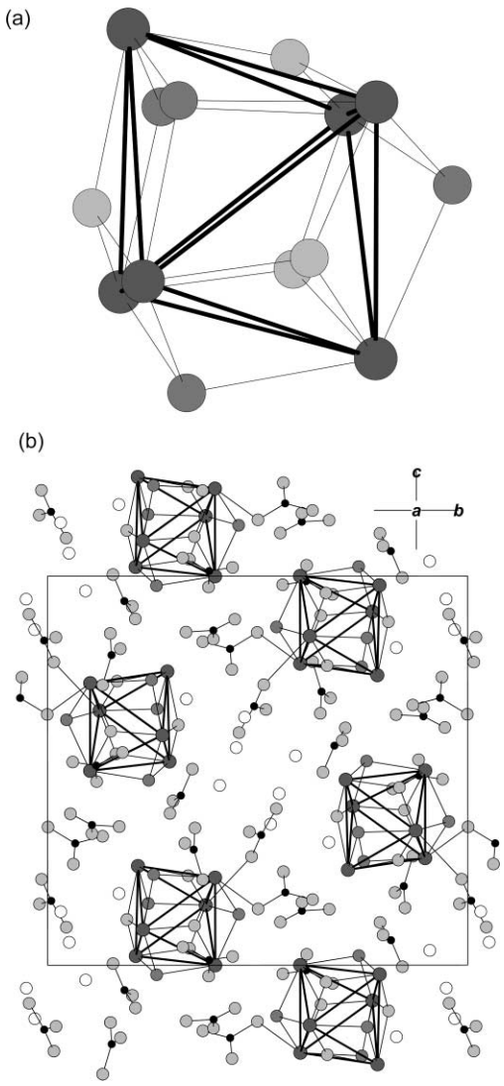

Fig. 1 (a) The crystal structure of $[Bi_6O_4(OH)_4](NO_3)_6{\cdot}4H_2O$, **C**, projected along [100]. (b) View showing how nitrate ions, water molecules and $Bi_6O_4(OH)_4$ polyhedra are placed in the unit cell. The complex ion $[Bi_6O_4(OH)_4]^{6+}$ has six bismuth atoms located at the corners of an nearly regular octahedron and eight oxygen atoms placed at the eight triangular faces. The four oxygens are almost coplanar with the three Bi atoms whereas the four hydroxyl oxygens have longer bond lengths to Bi and form a pyramidally coordination to Bi. Bi is shown as large size dark circles, oxygens as white (water), grey (oxygen in nitrate and coordinated to Bi) and dark (hydroxyl) circles. Nitrogen are small size black circles.

show pseudo-symmetry, and the crystals investigated are possibly multidomain twins.

TG–DTA investigations of the compounds **A**, **B** and **X** show that they all decompose in a number of steps with α-Bi_2O_3 as the end product around 610 °C. This investigation could possibly give an indication of the composition of the complex ions in the structure of **X** when the decomposition path of **X** was compared to those of **A** and **C**. The present *in-situ* investigation was made to study the decomposition paths of the basic bismuth(III) nitrates in detail and to further clarify the relationships between some of the compounds listed in Table 1.

Experimental

Chemistry

The chemicals used were $Bi(NO_3)_3{\cdot}5H_2O$ (BDH), urea, CH_4N_2O (Merck) and the basic bismuth(III) nitrates $[Bi_6O_5(OH)_3](NO_3)_5{\cdot}3H_2O$, **A**, $[Bi_6O_6(OH)_3](NO_3)_3{\cdot}1.5H_2O$, **B**, $[Bi_6O_4(OH)_4](NO_3)_6{\cdot}H_2O$, **D**, and $[Bi_6O_5(OH)_3](NO_3)_5{\cdot}2H_2O$, **X**, made as described previously.[1] Batch hydrothermal syntheses were performed in Teflon lined pressure vessels at temperatures up to 200 °C. Quantitative chemical analysis of bismuth in the compounds was made in complexometric titrations with . Nitrate was determined in micro Kjeldahl analysis, using a Tecator Kjeltec System 1002 Destilling Unit. This instrument was calibrated using mixtures of α-Bi_2O_3 (Fluka) and KNO_3 (Merck).[8,9] The results of the chemical analysis are listed in Table 2 and indicate for the compound **X** the composition $[Bi_6O_{4.5}(OH)_{3.5}](NO_3)_{5.5}{\cdot}H_2O$.

X-Ray powder diffraction

The purity of the reaction products from the batch hydrothermal synthesis was analysed by X-ray powder diffraction. X-ray powder diffractometry patterns were recorded at room temperature using a diffractometer (Model Stadi, Stoe, Darmstadt, Germany) with a position sensitive detector covering 40° in 2θ. Cu-Kα_1 was used (λ = 1.540598 Å), and the diffractometer was calibrated with a silicon standard (a = 5.43050 Å). Data were collected in transmission mode with samples mounted on Scotch tape. Powder patterns were also recorded with the same diffractometer in a step scan mode with steps of 1° in 2θ, using a linear position sensitive detector which covered 5° in 2θ. The recording time for a pattern covering 70° in 2θ was typically 21 h. In these measurements an external standard of Y_2O_3 (a = 10.60 Å) was used to calibrate the instrument. The compounds were identified from their powder patterns in the ICDD data base, see Table 1.

In-situ synchrotron X-ray powder diffraction studies on the hydrothermal reactions were carried out using a MAR-diffractometer at the X7B beam line at NSLS, Brookhaven National Laboratory. A reaction mixture of 300 mg solid and 1 mL of water was ground in a mortar and a fraction placed in a 0.7 mm diameter quartz glass capillary heated with hot air using a temperature ramp from 25 to 200 °C. The heating rate was typically 1.45 °C min^{-1}. The temperature of the hot air flow was measured with a chromel–alumel thermocouple and the hot air blower was calibrated by measurement of the melting point of sulfur housed in a capillary. An internal pressure of up to 1700 kPa from a nitrogen gas cylinder ensured that vapour bubbles did not form in the hydrothermal liquid. The wavelength used was λ = 0.90371 Å, determined from a powder pattern of LaB_6 (a = 4.156 Å). The MAR-diffractometer recorded a diffraction frame in 1.36 min, and with the temperature ramp described above, the 88 frames for this temperature range corresponded to ΔT = 2 °C per frame. The Bragg diffraction rings on the frames had diffraction spots from crystallites in the samples and were integrated into powder patterns with the software FIT2D.[10,11]

Solid-state thermal decomposition of the basic bismuth(III) nitrates were measured *in-situ* using an INEL-diffractometer and Co-Kα radiation (λ = 1.78897 Å). The diffractometer was calibrated with a sample of Y_2O_3 (a = 10.60 Å). The flat plate samples were heated on a platinum heating stage in a Model HTK-10 Anton-Paar GmbH, Graz, Austria, high temperature camera. The power to the heating element was controlled by a controller, Model HTK2-HC, Anton-Paar, with a Pt-10RhPt thermocouple welded to the back of the platinum heating element. Samples were placed using a pipette on the heating element as slurry of the solid in ethanol. After evaporation of the ethanol, the solid proved to have excellent physical contact to the sample holder, and temperature gradients in the samples were thus minimized. The *in-situ* experiments were made in the temperature range from 25 to 650 °C using a heating rate of typically 3.75 °C min^{-1}.

Thermogravimetric analysis

Thermogravimetric analyses were carried out on a Stanton Redcroft TGA-DTA simultaneous thermal analyser STA 1000/

Table 2 Results of chemical analysis

Compound	Mass loss[a] (%)	Bi (%)	NO_3^- (%)	Composition
D		70.44	20.9	$[Bi_6O_4(OH)_4](NO_3)_6 \cdot H_2O$
X1	4.70			
X2	10.23			
X3	14.36			
X4	17.75			
α-Bi_2O_3	21.53			Bi_2O_3
X		71.79	19.5	$[Bi_6O_{4.5}(OH)_{3.5}](NO_3)_{5.5} \cdot H_2O$
X1	3.64	73.98		
X2	8.32	78.05		
X3	11.78	81.42	9.10	
X4	15.90	85.22	5.40	
α-Bi_2O_3	20.14	89.70		Bi_2O_3
B		78.58	13.40	$BiOOH \cdot BiONO_3$
B1	2.27	80.43		
X3	2.83	80.74		
X4	5.87			
α-Bi_2O_3	11.07			Bi_2O_3
A		71.44	17.7	$[Bi_6O_5(OH)_3](NO_3)_5 \cdot 3H_2O$
A1	7.18	75.57		
A2	8.32	77.84		
X2				
X3	12.19			
X4	15.81			
α-Bi_2O_3	20.42			Bi_2O_3

[a] In solid-state synthesis from **D**, **X**, **B**, and **A**, respectively.

1500. Weight loss measurements were confirmed by large scale decomposition in platinum crucibles at temperatures up to 600 °C. The phase purity of the decomposition products was analysed by X-ray powder diffraction, and chemical analysis were made, see above.

Results and discussion

In-situ hydrothermal syntheses

Hydrolysis of $Bi(NO_3)_3 \cdot 5H_2O$. The X-ray powder diffraction patterns from the hydrolysis reaction of $Bi(NO_3)_3 \cdot 5H_2O$ under hydrothermal conditions are shown in Fig. 2. The initial hydrolysis product formed in mixing $Bi(NO_3)_3 \cdot 5H_2O$ with water is $[Bi_6O_4(OH)_4](NO_3)_6 \cdot 4H_2O$, **C**, and the sample contains **C** at hydrothermal conditions up to 70 °C, section #22, where $[Bi_6O_4(OH)_4](NO_3)_6 \cdot H_2O$, **D** is formed. At the formation of **D**, the background of the pattern is lowered (reduced) in agreement with the minor change in composition from **C** to **D**. This latter compound is stable up to 90 °C, section #33, where **X** is formed. **X** is then stable in this experiment at hydrothermal conditions up to 115 °C. The compound **X** is thus formed without urea in the reaction mixture.

Hydrolysis of $Bi(NO_3)_3 \cdot 5H_2O$ and urea. The X-ray powder diffraction patterns from the hydrolysis reactions of $Bi(NO_3)_3 \cdot 5H_2O$ in the presence of urea under hydrothermal conditions are shown in Fig. 3. Three crystalline compounds are seen in the temperature range 25 to 200 °C. The initial hydrolysis compound formed at 25 °C is **C**, and at 70 °C, section #22, this compound is converted to **X**, so the formation of **D** is not seen. This phase change is observed with a significant increase in the backgrounds of the powder patterns indicating a significant change in composition from **C** to **X**. A third compound is formed in the hydrothermal treatment via an amorphous phase at 110 to 120 °C, sections #42–47. This phase has a composition different from **X**, and its Bragg reflections are superimposed on patterns with high backgrounds. The phase is stable up to 200 °C, and it is identified as $Bi_2O_2CO_3$. The urea is therefore decomposed to CO_2 and NH_3 at 120 °C.

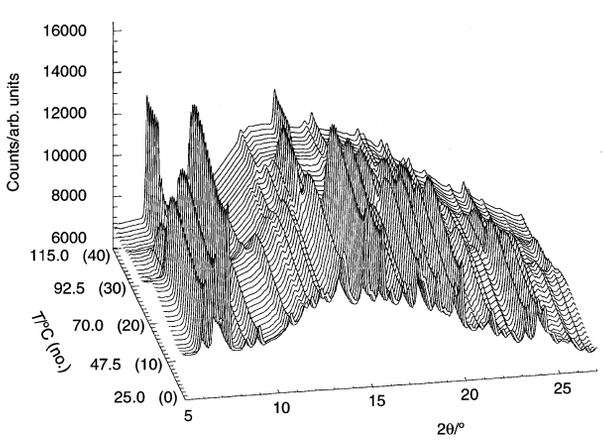

Fig. 2 Stack of powder patterns showing the patterns of **C**, **D** and **X** in the temperature range 25–115 °C.

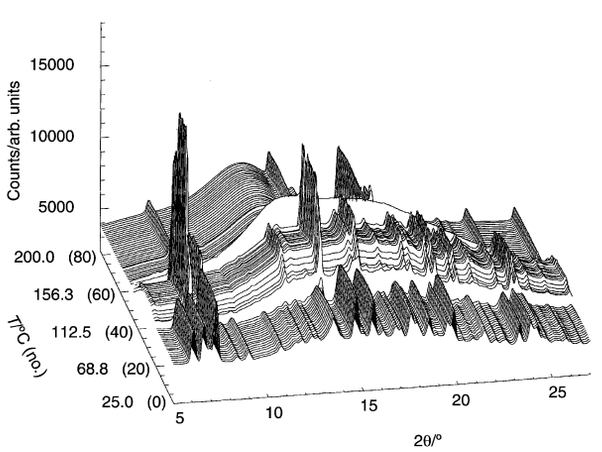

Fig. 3 Stack of powder patterns showing the patterns of **C**, **X** and $Bi_2O_2CO_3$ in the temperature range 25–200 °C.

Hydrolysis of $[Bi_6O_5(OH)_3](NO_3)_5\cdot 3H_2O$, A. The powder patterns are displayed in Fig. 4 showing three crystalline phases. The compound **A** is stable at hydrothermal conditions up to 120 °C, section #43, where a new phase, designated **AB** (composition not known), is formed. The backgrounds of the patterns is at first reduced but at higher temperatures increased significantly. The new phase has a Bragg reflection at $2\theta = 2.55°$ (λ = 0.90371 Å) with d = 20.3 Å. This phase is consumed at 160 °C, section #62, where **B** is formed as a pure phase. The backgrounds of the patterns with **B** are higher than for the patterns at the start of the experiment, indicating also the presence of some amorphous bismuth compound.

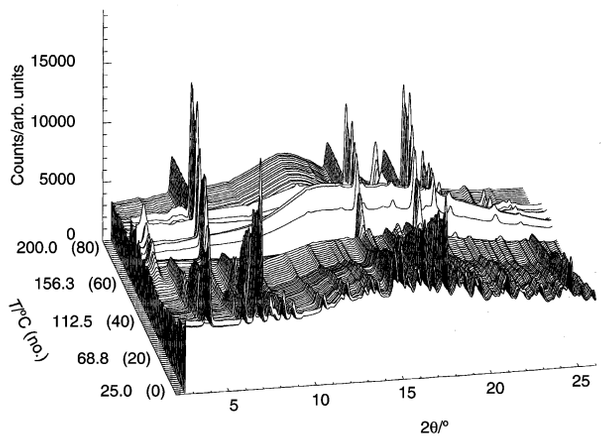

Fig. 4 Stack of powder patterns showing the patterns of **A**, **AB** (composition not known) and **B** in the temperature range 25–200 °C.

The hydrothermal formation of **B** from **A** was also observed previously[1] in batch syntheses.

Hydrolysis of $[Bi_6O_4(OH)_4](NO_3)_6\cdot H_2O$, D. The sample contained **D** with an impurity of **A** and the powder patterns from the hydrothermal treatments are displayed in Fig. 5. On heating the quantity of **A** increases and that of **D** decreases, and at 70 °C, section #20, the sample contained **A** only. Simultaneously, the background of the patterns has increased, indicating a significant change in the composition from **D** to **A** and the possible formation of some amorphous material. At 86 °C, section #28, **A** is then converted to **X** and this compound then remains stable in the experiment until 200 °C. At 120 °C a significant increase in the backgrounds of the patterns is observed, without a significant increase in the intensities of the Bragg reflections. This is possibly due to crystal growth of **X** and an increased water : solid ratio of the sample in the X-ray beam. The two *in-situ* hydrothermal experiments with **A** and **D** were

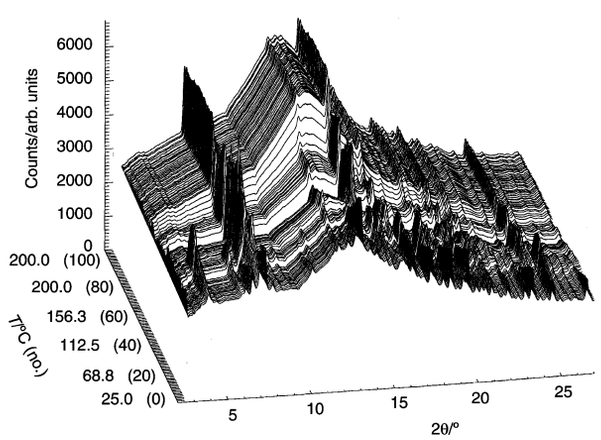

Fig. 5 Stack of powder patterns showing the patterns of **D**, **A** and **X** in the temperature range 25–200 °C.

Table 3 Experimental conditions and results in batch hydrothermal synthesis

No.	Solid(s)/g	$V(H_2O)$/mL	T/°C	t/h	Product
$Bi(NO_3)_3\cdot 5H_2O$					
1	0.3	2	75	92	**X**
2	0.3	4	75	44	**A**
3	0.3	4	100	70	**A**
$Bi(NO_3)_3\cdot 5H_2O$ + urea					
4	0.3	2	75	92	**A**
5	0.3	4	75	44	**A**
6	0.3	4	100	70	$Bi_2O_2CO_3$
D + **A**					
7	0.3	4	100	20	**B**
8	0.3	4	180	20	**B**

made with the crystalline solids and pure water. The liquid medium has a much higher pH value than the liquids in the hydrothermal experiments with $Bi(NO_3)_3\cdot 5H_2O$, where pH < 1. This may explain the different reaction routes in the four experiments.

Batch hydrothermal synthesis. Batch hydrothermal syntheses were made to verify the results obtained in the *in-situ* experiments, and the experimental conditions and results are listed in Table 3. Experiment 1 confirms the formation of **X** in the absence of urea.

In-situ X-ray diffraction, solid-state reactions

Thermal decomposition has been reported previously of basic bismuth(III) nitrates,[7] and powder patterns of two phases obtained at 320 and at 485 °C, respectively, have been reported. The pattern of the 320 °C phase is possibly not a pattern of a pure phase. The 485 °C phase was obtained in a previous investigation[1] and the pattern of the phase was indexed on a monoclinic cell (Table 6 of ref. 1). The observed temperatures for the phase changes in the present investigation were subsequently used in solid-state batch syntheses to obtain the pure phases in the decomposition steps. Bismuth and in some cases nitrate chemical analyses were made of the decomposition products, and the X-ray powder patterns were recorded using Cu-Kα_1 radiation. The powder patterns refer to the products of these batch syntheses. The Figures of these powder patterns and the TGA diagrams mentioned below (Figs. S1–8) are deposited as ESI. †

$[Bi_6O_4(OH)_4](NO_3)_6\cdot H_2O$, D. The sample was heated from 20 to 650 °C at a heating rate of 3.75 °C min^{-1}. Phase changes were observed at 145, 225, 325, 475 and 520 °C, where the final product formed was α-Bi_2O_3. These temperatures are marked in the TG–DTA diagram, Fig. S1, which has minima in the DTA-curve at 183, 305, 340, 500 and 567 °C, respectively. The phases found in the temperature intervals were: **D**, 25–145 °C; **X1**, 145–225 °C; **X2**, 225–325 °C; **X3**, 325–475 °C; **X4**, 475–520 °C; α-Bi_2O_3, 520–650 °C. Fig. S2, ESI, † displays the powder patterns of these compounds and Table 4 lists the powder pattern of the phase **X3**.

$[Bi_6O_5(OH)_3](NO_3)_5\cdot 2H_2O$, X. The sample was heated from 20 to 600 °C at a heating rate of 1.24 °C min^{-1}. Phase changes were observed at 250, 320, 400, 510 and 560 °C, respectively. These temperatures are marked in the TG–DTA diagrams, Fig. S3, ESI, † which show minima at 342, 454, 510 and 573 °C, respectively. The corresponding phases are: **X**, 25–250 °C; **X1**, 250–320 °C; **X2**, 320–400 °C; **X3**, 400–510 °C; **X4**, 510–560 °C; α-Bi_2O_3, 560–600 °C. Fig. S4, ESI, † displays the powder patterns of these compounds.

Table 4 Powder pattern of the decomposition product **X3**, indexed on a monoclinic unit cell: a = 9.83(2), b = 5.88(1), c = 4.08(1) Å, β = 91.7(1)°. Figure of merit, $M(11)$ = 12.8 (λ = 1.540598 Å)

$2\theta_{obs}$/°	$2\theta_{calc}$/°	d_{obs}/Å	d_{calc}/Å	I_{obs}	h	k	l
8.95	8.99	9.873	9.827	16	1	0	0
23.83	23.84	3.731	3.730	6	1	0	1
28.30	28.30	3.151	3.151	100	1	1	1
31.85	31.93	2.807	2.801	42	2	1	−1
34.64	34.59	2.587	2.591	8	3	0	−1
41.20	41.20	2.189	2.190	7	3	2	0
45.65	45.65	1.986	1.986	11	1	0	2
47.73	47.74	1.904	1.901	8	2	0	−2
54.60	54.64	1.679	1.678	14	5	1	1
58.43	58.44	1.578	1.578	6	6	1	0
66.57	66.56	1.404	1.404	3	1	3	−2

$[Bi_6O_6(OH)_3](NO_3)_3\cdot 1.5H_2O$, B. The sample was heated from 20 to 650 °C at a heating rate of 3.75 °C min^{-1}, and phase changes were observed at 320, 430, 510 and 540 °C. These temperatures are marked in the TG–DTA diagram, Fig. S5, ESI,† which has minima at 365, 543, 562 and 592 °C, respectively. The phases found are: **B**, 25–320 °C; **B1**, 320–430 °C; **X3**, 430–510 °C; **X4**, 510–540 °C; α-Bi_2O_3, 540–650 °C. Fig. S6, ESI,† displays the powder patterns of these compounds.

$[Bi_6O_5(OH)_3](NO_3)_5\cdot 3H_2O$, A. The sample was heated from 20 to 600 °C using a heating rate of 3.75 °C min^{-1}. Phase changes were observed at 50, 75, 150, 300, 420, 473 and 575 °C. These temperatures are marked in the TG–DTA diagram, Fig. S7, ESI,† which has minima at 125, 306, 345, 455, 520 and 577 °C. The phases found are: **A**, 25–50 °C; a phase with a powder pattern that resembles **A**, 50–75 °C; a phase with a powder pattern that resembles **D**, 75–150 °C; **A1**, 150–300 °C; **A2**, 300–420 °C; **X3**, 420–473 °C; **X4**, 473–575 °C; α-Bi_2O_3, 575–600 °C. Fig. S8, ESI,† displays the powder patterns of these compounds.

Analysis of X-ray diffraction data

The powder patterns displayed in Figs. S1, S3, S5 and S7 (ESI†) show that the decomposition products formed at relatively low temperatures have broad Bragg peaks. For this reason it was only possible to index the product **X3** using the program DICVOL,[12] and the results are listed in Table 4. Indexed synchrotron X-ray powder patterns of **X4**, **B** and **X** are reported in ref. 1 as Tables 6, 5 and 3, respectively. The full pattern of **X** has been used in attempts to get structural models for this compound. The compound contains Bi as the dominating scattering atom, and the composition is only partly known. The efforts have been limited to models suggesting positions for Bi-atoms. The direct method program EXPO was used.[13]

Calculations for phase **X** was made using the unit cell a = 15.185(1), c = 15.834(2) Å and space group $R\bar{3}$. The expected number of Bi atoms in this cell is 36. Two Bi atoms were found in site 18*f* at the coordinates 0.6659, 0.1986, 0.2370, and 0.6656, 0.1966, 0.7377, corresponding to six Bi_6 octahedra with Bi–Bi distances of 3.6 Å as found in the structures of **C** and **D**.

Conclusion

The *in-situ* hydrothermal synthesis and the batch hydrothermal syntheses show that the compound **X** can be obtained without the homogeneous hydrolysis of urea, and that it is formed from **C** or **D**. The *in-situ* solid-state decomposition synthesis shows that **X** is formed from **D**, and that the compounds **X** and **D** follow the same decomposition pattern with the sequence **X1**, **X2**, **X3**, **X4** to α-Bi_2O_3 (Figs. S1 and S3). These compounds have increasing Bi contents and decreasing NO_3 contents. The chemical analysis shows that **X** has a higher NO_3 content than **A** and a smaller content than that of **D**, and **X** shows a smaller loss in weight than **D**. The chemical analysis supports the composition $[Bi_6O_{4.5}(OH)_{3.5}](NO_3)_{5.5}\cdot H_2O$ for **X**. The formula $[Bi_6O_5(OH)_3](NO_3)_5\cdot 2H_2O$ for **X**, which has previously been reported, is thus most likely in error. Attempts to solve the crystal structure of **X** in a single crystal analysis failed, possibly because the crystals investigated were all twinned. Structure analysis of the synchrotron X-ray diffraction data of **X** suggests that Bi-atoms are placed in Bi_6 octahedra. It is thus assumed that the crystals of **X** contain coordination polyhedra with a geometry similar to the ions in the crystals of **C** and **D**. The previous ^{1}H MAS NMR spectra of **A** and **X** suggested that both compounds contained hydroxyl groups and water molecules.[1]

The compounds **A** and **B** have different decomposition paths in the low temperature range than **C**, **D** and **X** but do form the compounds **X3** and **X4** from 420 and 430 °C, respectively, to α-Bi_2O_3. Compound **A** contains the ion $[Bi_6O_5(OH)_3]^{5+}$ in the complex ion $\{[Bi_6O_5(OH)_3]^{5+}\}_2$, and it is thus understandable that its decomposition path in the low temperature range is different from those of **C**, **D** and **X**. All the compounds investigated **A**, **B**, **C**, **D** and **X** have the same final decomposition products: **X3**, **X4** and α-Bi_2O_3.

Acknowledgements

The Danish Natural Science Research Council and Aarhus University Research Foundation have supported this investigation with grants. T. R. J. is grateful for a Steno Stipend. Carlsbergfondet is acknowledged for financial support by purchase of furnace equipment and the TG–DTA thermal analyser. The synchrotron X-ray measurements were carried out at Brookhaven National Laboratory, supported under contract DE-AC02-98CH10886 with the US Department of Energy by its Division of Chemical Sciences Office of Basic and Energy Science. Mrs C. Secher, Mrs B. Lundtoft, and Mr N. J. Hansen are thanked for valuable assistance.

References

1 A. N. Christensen, M.-A. Chevallier, J. Skibsted and B. B. Iversen, *J. Chem. Soc., Dalton Trans.*, 2000, 265.
2 F. Lazarini, *Acta Crystallogr., Sect. B*, 1978, **34**, 3169.
3 F. Lazarine, *Cryst. Struct. Commun.*, 1979, **8**, 69.
4 B. Sundvall, *Acta Chem. Scand., Ser. A*, 1979, **33**, 219.
5 F. Lazarine, *Acta Crystallogr., Sect. B*, 1979, **35**, 448.
6 G. Gattow and D. Schott, *Z. Anorg. Allg. Chem.*, 1963, **324**, 31.
7 B. S. Brcic, D. Kolar, F. Lazarine and M. Malesic, *Monatsh. Chem.*, 1973, **104**, 365.
8 *Complexometric Assay Methods with Triplex*, E. Merck, Darmstadt, 3rd edn.
9 *DS 230: Water Quality-Nitrate-Nitrite Nitrogen-Reduction by Devardas Alloy*, Dansk Standardiseringsråd, Postboks 77, DK-2900 Hellerup, Denmark, 1975.
10 A. P. Hammersley, ESRF Internal Report, ESRF98HA01T, FIT2D V9. 129, Reference Manual V3.1, 1998.
11 A. P. Hammersley, S. O. Svensson, M. Hanfland, A. N. Fitch and D. Häuserman, *High Pressure Res.*, 1996, **14**, 235.
12 A. Boultif and D. Loüer, *J. Appl. Crystallogr.*, 1991, **24**, 987.
13 A. Altomare, M. C. Burla, G. Cascarano, C. Giacovazzo, A. Guagliardi, A. G. C. Moliterni and G. Polidori, *J. Appl. Crystallogr.*, 1995, **28**, 842.